Coupling between splay deformations and density modulations in splay-bend phases of bent colloidal rods

SUPPLEMENTAL MATERIAL

Carmine Anzivino,[1,*] René van Roij,[2] and Marjolein Dijkstra[1,†]

[1] *Soft Condensed Matter, Debye Institute for Nanomaterials Science, Utrecht University, Princetonplein 1, 3584 CC Utrecht, The Netherlands*

[2] *Institute for Theoretical Physics, Utrecht University, Princetonplein 5, 3584 CC Utrecht, The Netherlands*

(Dated: January 28, 2022)

I. THEORY

As discussed in the main text, we extended the theory introduced in Ref. [1] by considering a z-dependent nematic order parameter $S(z)$ in the definition of the tensorial order parameter $\mathbf{Q}$ as well as a z-dependent magnitude $P(z)$ in the definition of the polarization vectors $\mathbf{P}_{\rm TB}$ and $\mathbf{P}_{\rm SB}$. It follows that, after insertion of $\mathbf{Q}$ and $\mathbf{P}$, the grand potential $\Delta\Omega$ at fixed chemical potential μ becomes a function of the wave number q and the tilt angle θ as well as a functional of $S(z)$ and $P(z)$, i.e.

$$\Delta\Omega(\mathbf{Q},\mathbf{P}) \equiv \Delta\Omega\big(\mu; q, \theta, [S,P]\big). \tag{S1}$$

To fully minimize $\Delta\Omega$ we adopt the following protocol. We first fix the chemical potential μ and the wave number q, and solve the system of Euler-Lagrange equations

$$\frac{\delta\Delta\Omega}{\delta S(z)} = \partial_z \frac{\delta\Delta\Omega}{\delta(\partial_z S(z))}; \quad \frac{\delta\Delta\Omega}{\delta P(z)} = \partial_z \frac{\delta\Delta\Omega}{\delta(\partial_z P(z))}, \tag{S2}$$

for several values of the tilt angle θ. We repeat this procedure for several values of q, while keeping μ fixed. In this way we identify the grand-potential minimum of the $N_{\rm TB}$ phase characterized by $q_{\rm TB}(\mu), \theta_{\rm TB}(\mu), S_{\rm TB}(\mu;z)$ and $P_{\rm TB}(\mu;z)$, and of the $N_{\rm SB}$ phase described by $q_{\rm SB}(\mu), \theta_{\rm SB}(\mu), S_{\rm SB}(\mu;z)$ and $P_{\rm SB}(\mu;z)$. As stated in the main text, we keep the coefficients $a = 1.436, b = 5.851, d = 3.693$ and $\beta\mu^* = 6.855$ fixed in order to describe the "Onsager"-type I-N phase transition of uniaxial hard needles occurring at $\beta\mu_{IN} = \beta\mu^* - b^2/(4ad) = 5.241$ [1, 2]. Furthermore we set $e_2 = 1, S_0 = 0.99, e_4 = 0.5, \kappa = 0.3L^2$, and $\lambda = 0.18$, while we vary l_1 and l_2 to change the ratio between the splay and twist elastic constants K_{11} and K_{22}.

We first consider the case $l_1 = 0.165L^2$ and $l_2 = 0.427L^2$, from which $K_{11}/K_{22} = 1 + l_2/(2l_1) = 2.294$. In Fig. S1 we plot $\Delta\Omega_{\rm TB}/V$ as a function of the tilt angle θ for several values of the wave number q, at fixed values of the chemical potential μ. We identify the grand-potential minima for each μ, and find that the corresponding q and θ coincide with $q_{\rm TB}$ and $\theta_{\rm TB}$ obtained in Ref. [1], given by

$$q_{\rm TB}(\mu;S,P) = -\frac{3\lambda\sin(2\theta_{\rm TB})SP}{8\kappa P^2 + 4S^2(2l_1+l_2)\sin^2\theta_{\rm TB} - 4S^2 l_2 \sin^4\theta_{\rm TB}}, \tag{S3}$$

and

$$\sin^2\theta_{\rm TB}(\mu;S,P) = -\frac{\kappa P^2}{S^2 l_1} + \frac{\sqrt{\kappa P^2(\kappa P^2 + S^2 l_1)}}{S^2 l_1}, \tag{S4}$$

respectively. In a similar way, we determine the grand-potential minima of the $N_{\rm SB}$ phases (not shown here). In Fig. S2(a) we plot the resulting grand-potential densities of the $N_{\rm TB}$ and $N_{\rm SB}$ phases, respectively, as a function

*Present Address: Department of Physics "A. Pontremoli", University of Milan, via Celoria 16, 20133 Milan, Italy; Electronic mail: carmine.anzivino@gmail.com

†Electronic mail: m.dijkstra@uu.nl

of the chemical potential μ. We define the grand-potential densities of the $N_{\rm TB}$ and $N_{\rm SB}$ phases as $\Delta\bar{\Omega}_{\rm TB}/V \equiv \Delta\Omega_{\rm TB}/V - \Delta\Omega_N/V$ and $\Delta\bar{\Omega}_{\rm SB}/V \equiv \Delta\Omega_{\rm SB}/V - \Delta\Omega_N/V$, respectively, where $\Delta\Omega_N/V$ is the grand-potential density of the (metastable) uniaxial N phase. We find that $\Delta\bar{\Omega}_{\rm TB}/V$ and $\Delta\bar{\Omega}_{\rm SB}/V$ exactly coincide with the grand potential densities of the $N_{\rm TB}$ and $N_{\rm SB}$ phases obtained when S and P are assumed to be z-independent in the $\mathbf{Q}$ and $\mathbf{P}$ order parameters, respectively [1]. We observe that $\Delta\Omega_{\rm TB} < \Delta\Omega_{\rm SB}$ at each $\beta\mu \geq \beta\mu_{NN_{\rm TB}} = 5.663$ and that $\Delta\bar{\Omega}_{\rm TB} = 0$ at the critical chemical potential $\beta\mu_{NN_{\rm TB}}$. It follows from Fig. S2(a) that a second-order N-$N_{\rm TB}$ phase transition takes place at $\beta\mu_{NN_{\rm TB}}$. Furthermore, Fig. S3 shows that the renormalized bend elastic constant $K_{33}^{\rm eff}$, as defined in Ref. [1], vanishes at $\beta\mu_{NN_{\rm TB}}$. As noticed in the main text and shown in Figs. S4(a) and S4(b), $S_{\rm TB}(z)$ and $P_{\rm TB}(z)$ are constant along z for each μ. As a consequence, the corresponding density profile $c_{\rm TB}$ as shown in Fig. S4(c) is also a spatial constant. We plot the extremal solutions $S_{\rm TB}$ and $P_{\rm TB}$ (with points) as a function of μ in Figs. S5(a) and S5(b), respectively, and find that they exactly coincide with those (plotted with full lines) obtained in Ref. [1], by assuming that S and P are z-independent in the $\mathbf{Q}$ and $\mathbf{P}_{\rm TB}$ order parameters, respectively. In particular $S_{\rm TB}(\mu)$ coincides with $S_N(\mu)$ of Eq. (3) of the main text.

Subsequently, we consider the case $l_1 = 0.1L^2$ and $l_2 = 0.0427L^2$, from which $K_{11}/K_{22} = 1 + l_2/(2l_1) = 1.124$. We identify the grand-potential minima of the $N_{\rm TB}$ and $N_{\rm SB}$ phases for each μ. In Fig. S6 we exemplarily plot $\Delta\Omega_{\rm SB}/V$ as a function of the tilt angle θ for several values of the wave number q, at fixed values of the chemical potential μ, from which we determine the minimal grand potential. In Fig. S2(b) we plot $\Delta\bar{\Omega}_{\rm TB}/V$ and $\Delta\bar{\Omega}_{\rm SB}/V$ as a function of $\beta\mu$. Again we find that $\Delta\bar{\Omega}_{\rm TB}/V$ and $\Delta\bar{\Omega}_{\rm SB}/V$ exactly coincide with the grand potential densities of the $N_{\rm TB}$ and $N_{\rm SB}$ phases obtained when S and P are assumed to be z-independent in the $\mathbf{Q}$ and $\mathbf{P}$ order parameters, respectively [1]. We observe that, this time, $\Delta\Omega_{\rm TB} > \Delta\Omega_{\rm SB}$ at each $\beta\mu \geq \beta\mu_{NN_{\rm SB}} = 5.354$ and that $\Delta\bar{\Omega}_{\rm SB} = 0$ at $\beta\mu_{NN_{\rm SB}}$. It follows that a second-order N-$N_{\rm SB}$ phase transition takes place at $\beta\mu_{NN_{\rm SB}}$. As shown in Fig. S3, $\beta\mu_{NN_{\rm SB}}$ is also the point where the renormalized bend elastic constant $K_{33}^{\rm eff}$, as defined in Ref. [1], vanishes.

As noticed in the main text, $S_{\rm SB}$ and $P_{\rm SB}$ display periodic modulations along z for $\mu > \mu_{NN_{\rm SB}}$. In Fig. 1(c) we plot with points the period-average of the profiles $S_{\rm SB}$ and $P_{\rm SB}$ as a function of μ. We find that these period-average values exactly coincide with the extremal solutions $S_{\rm TB}$ and $P_{\rm TB}$ (plotted with full lines) obtained in Ref. [1], by assuming that S and P are z-independent in the $\mathbf{Q}$ and $\mathbf{P}_{\rm SB}$ order parameters, respectively. In particular, the spatial average of $S_{\rm SB}(\mu; z)$ coincides with the $S_N(\mu)$ of Eq. (3) (denoted by the dashed line) for sufficiently low $\beta\mu$. For high $\beta\mu$, we find that the period-average $S_{\rm SB}(\mu; z)$ deviates slightly from $S_N(\mu)$ of Eq. (3) due to the small-θ approximation employed in the computation of $\Delta\Omega_{\rm SB}/V$ [1]. Finally, in Fig. S6 we plot $\Delta\Omega_{\rm SB}/V$ as a function of the tilt angle θ for several values of the wave number q, at fixed values of the chemical potential μ. We observe that, for each μ, the minimum values of q and θ coincide with $q_{\rm SB}$ and $\theta_{\rm SB}$ as obtained in Ref. [1], given by

$$q_{\rm SB}(\mu; S, P) = \frac{3\lambda\theta_{\rm SB}(\theta_{\rm SB}^2 - 8)PS}{8(4 + 3\theta_{\rm SB}^2)\kappa P^2 + 16S^2(2l_1 + l_2)\theta_{\rm SB}^2}, \tag{S5}$$

and

$$\theta_{\rm SB}^2(\mu; S, P) = \frac{16\kappa P^2}{3\kappa P^2 + \sqrt{\kappa P^2(57\kappa P^2 + 32S^2(2l_1 + l_2))}}, \tag{S6}$$

respectively, where S and P are the period-average of the $S_{\rm SB}(z)$ and $P_{\rm SB}(z)$ profiles, at each μ.

II. COUPLING BETWEEN SPLAY DEFORMATIONS AND DENSITY MODULATIONS

As shown in Fig. S9, the $S_{\rm SB}(z)$ profiles accurately fit the functional form

$$S_{\rm SB}(z) = S_{\rm SB}^{\rm max} \cos\big(\theta_S \sin\big(q_{\rm SB} z\big)\big), \tag{S7}$$

where the fit parameter θ_S is reported for several $\Delta\mu$ in Table S1. In Fig. S10 we plot $S_{\rm SB}(\nabla\cdot\hat{\mathbf{n}}_{\rm SB})$ and $H(\nabla S_{\rm SB})\cdot\hat{\mathbf{n}}_{\rm SB}$ as a function of z, with full and dashed lines, respectively. The figure shows that a spatial constant H can be found, at each μ, such that

$$S_{\rm SB}(\nabla\cdot\hat{\mathbf{n}}_{\rm SB}) = H(\nabla S_{\rm SB})\cdot\hat{\mathbf{n}}_{\rm SB}. \tag{S8}$$

$10^2\beta\Delta\mu$	θ_S
0.0	0.0
0.1	0.0022010
0.2	0.0036504
0.3	0.0050369
0.4	0.0062674
0.5	0.0074497
1.0	0.0127617
2.0	0.021850

TABLE S1: Coefficients θ_S of the functional form Eq. (S7) for varying chemical potentials $\Delta\mu \equiv \mu - \mu_{NN_{\rm SB}}$, obtained through fitting the $S_{\rm SB}(z)$ profiles (see Figs. 1(a) and S9).

By using the thermodynamic identity (6), we can write

$$\begin{aligned}\frac{\nabla S_{\rm SB}}{S_{\rm SB}} &= \frac{2S_{\rm SB}(\nabla S_{\rm SB})}{2S_{\rm SB}^2} \\ &= \frac{\nabla S_{\rm SB}^2}{2S_{\rm SB}^2} \\ &= \frac{\nabla\left(\frac{c_{\rm SB}(z)-c_I}{a}\right)}{2\frac{c_{\rm SB}(z)-c_I}{a}} \\ &= \frac{\nabla c_{\rm SB}(z)}{2\big(c_{\rm SB}(z)-c_I\big)}.\end{aligned} \tag{S9}$$

Inserting (S9) into (S8) we find Eq. (8).

[1] C. Anzivino, R. van Roij, and M. Dijkstra, The Journal of Chemical Physics **152**, 224502 (2020).
[2] J. C. Everts, M. T. J. J. M. Punter, S. Samin, P. van der Schoot, and R. van Roij, The Journal of Chemical Physics **144**, 194901 (2016).

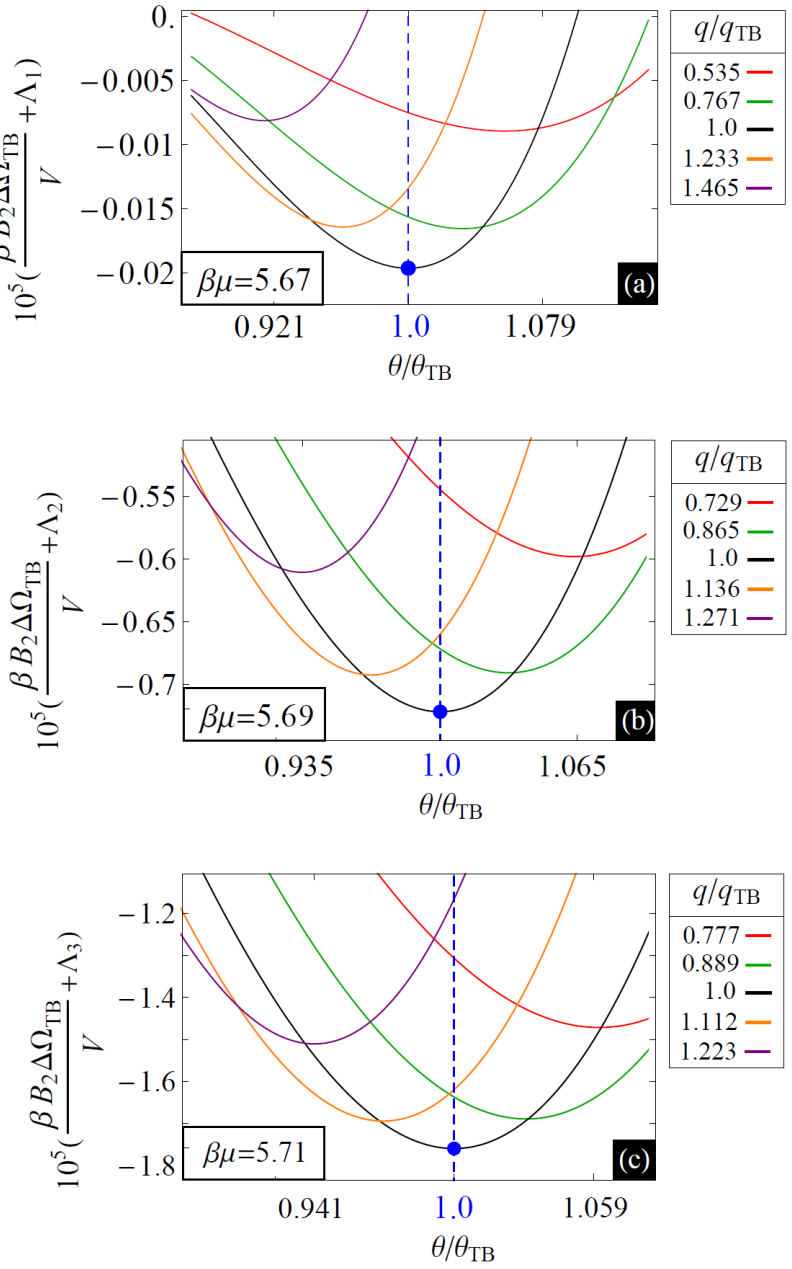

FIG. S1: $\Delta\Omega_{\rm TB}/V$ as a function of the tilt angle θ for several values of the wave number q, in the case of $\beta\mu = 5.67$ (a), $\beta\mu = 5.69$ (b) and $\beta\mu = 5.71$ (c). We consider the coefficients $l_1 = 0.165L^2, l_2 = 0.427L^2, e_2 = 1, S_0 = 0.99, e_4 = 0.5, \kappa = 0.3L^2$ and $\lambda = 0.18L^2$. We observe that, at each μ, the minimum values of q and θ correspond to the $q_{\rm TB}$ and $\theta_{\rm TB}$ of Eqs. (S3) and (S4), respectively. In (a), (b), and (c) we plot $\Delta\Omega_{\rm TB}/V$ subtracted by the irrelevant constant values $\Lambda_1 = 0.4729, \Lambda_2 = 0.4987$, and $\Lambda_3 = 0.5248$, respectively.

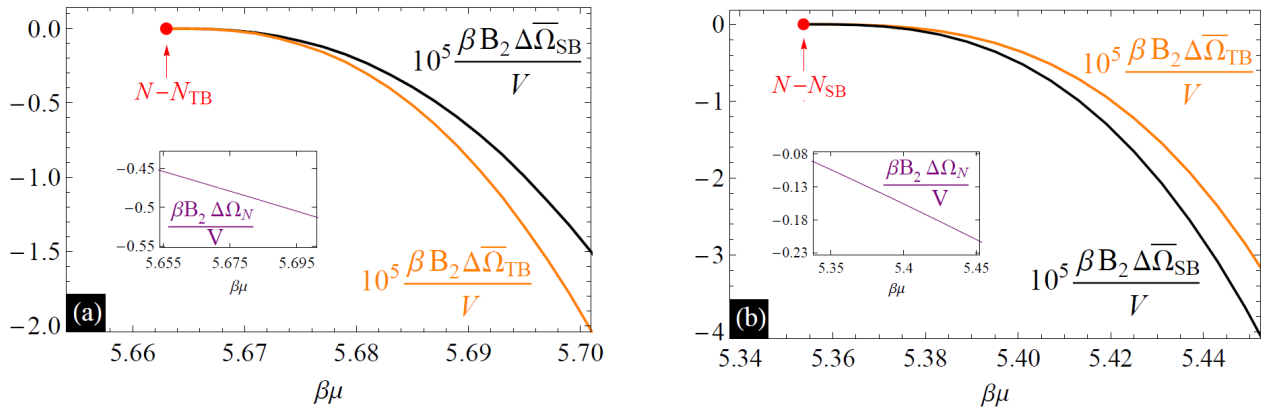

FIG. S2: Grand-potential density of the $N_{\rm TB}$ phase $\Delta\bar{\Omega}_{\rm TB}/V \equiv \Delta\Omega_{\rm TB}/V - \Delta\Omega_N/V$ and of the $N_{\rm SB}$ phase $\Delta\bar{\Omega}_{\rm SB}/V \equiv \Delta\Omega_{\rm SB}/V - \Delta\Omega_N/V$, as a function of the chemical potential $\beta\mu$, for the Landau coefficients $l_1 = 0.165L^2$ and $l_2 = 0.427L^2$ (a), and $l_1 = 0.1L^2$ and $l_2 = 0.0427L^2$ (b). In (a) $K_{11}/K_{22} = 2.294$, while in (b) $K_{11}/K_{22} = 1.214$. The other coefficients are $e_2 = 1, S_0 = 0.99, e_4 = 0.5, \kappa = 0.3L^2$ and $\lambda = 0.18L^2$ in all cases. Either in (a) and in (b) the grand-potential density $\Delta\Omega_N/V$ of the uniaxial N phase is plotted in the inset. In case (a) a N-$N_{\rm TB}$ transition occurs at $\beta\mu_{NN_{\rm TB}} = 5.663$, in case (b) a N-$N_{\rm TB}$ transition occurs at $\beta\mu_{NN_{\rm SB}} = 5.354$.

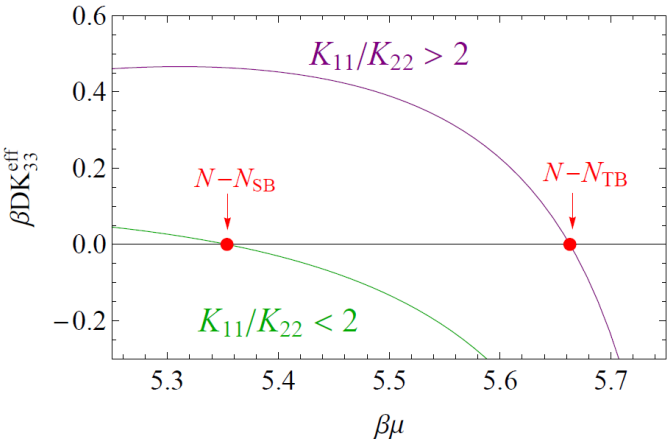

FIG. S3: Renormalized bend elastic constat $K_{33}^{\rm eff}$ (defined in Ref. [1]) as a function of the chemical potential $\beta\mu$, for the Landau coefficients $l_1 = 0.165L^2$ and $l_2 = 0.427L^2$ (violet), and $l_1 = 0.1L^2$ and $l_2 = 0.0427L^2$ (green). The other coefficients are $e_2 = 1, S_0 = 0.99, e_4 = 0.5, \kappa = 0.3L^2$ and $\lambda = 0.18L^2$ in all cases. In the former case $K_{33}^{\rm eff}$ vanishes at the chemical potential $\beta\mu_{\rm TB} = 5.663$, where a second-order N-$N_{\rm TB}$ transition occurs. In the latter case $K_{33}^{\rm eff}$ vanishes at the chemical potential $\beta\mu_{\rm SB} = 5.354$, where a second-order N-$N_{\rm SB}$ transition occurs.

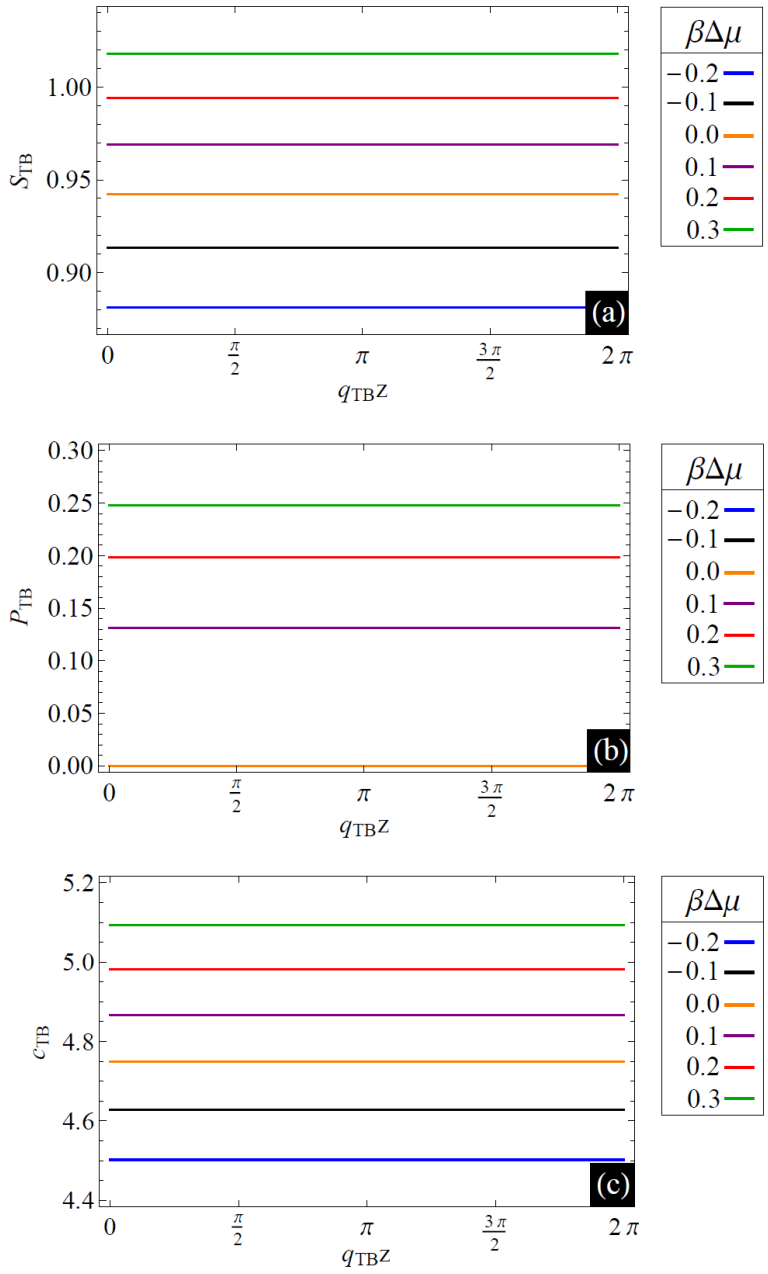

FIG. S4: Nematic order parameter S_{TB} (a), amplitude of the polarity P_{TB} (b), and particle concentration c_{TB} (c), in the N_{TB} phase, as a function of z for several values of $\Delta\mu \equiv \mu - \mu_{NN_{\mathrm{TB}}}$, and for the coefficients $l_1 = 0.165L^2, l_2 = 0.427L^2, e_2 = 1, S_0 = 0.99, e_4 = 0.5, \kappa = 0.3L^2$ and $\lambda = 0.18L^2$. We observe that $S_{\mathrm{TB}}, P_{\mathrm{TB}}$ and c_{TB} remain constant along z for each μ.

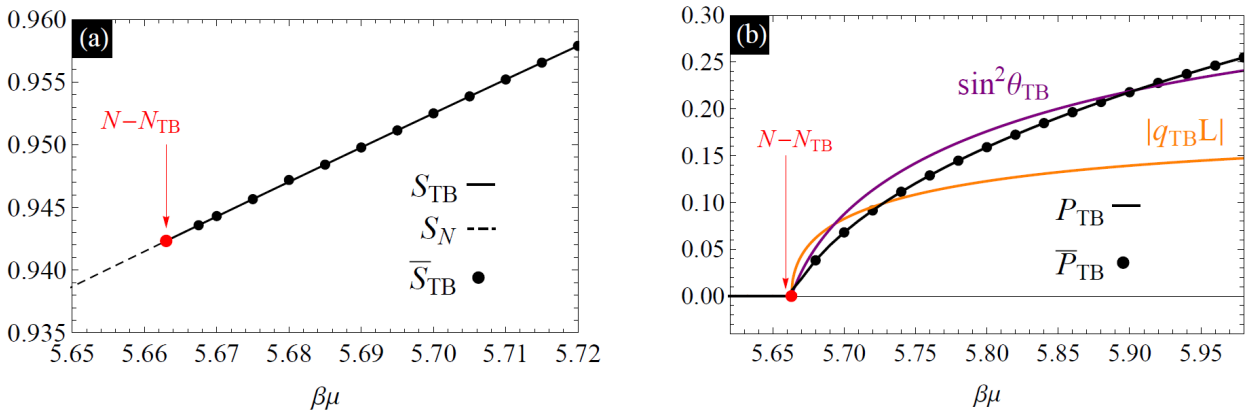

FIG. S5: Scalar nematic order parameter $S_{\rm TB}$ (a) and amplitude of the polarity $P_{\rm TB}$ (b) in the $N_{\rm TB}$ phase as a function of the chemical potential $\beta\mu$, for the coefficients $e_2 = 1.0, e_4 = 0.5, \lambda = 0.18L, \kappa = 0.3L^2, S_0 = 0.99, l_1 = 0.165L^2$ and $l_2 = 0.427L^2$. Full lines and points represent solutions obtained when S and P are assumed z-independent and z-dependent in the $\mathbf{Q}$ and $\mathbf{P}_{\rm TB}$ order parameters, respectively. A perfect match is found. In particular, $S_{\rm TB}$ corresponds to $S_N(\mu)$ of Eq. (3). In (b) we also plot the equilibrium wave vector $q_{\rm TB}$ and tilt angle $\theta_{\rm TB}$ as given by Eqs. (S3) and (S4), respectively as a function of $\beta\mu$.

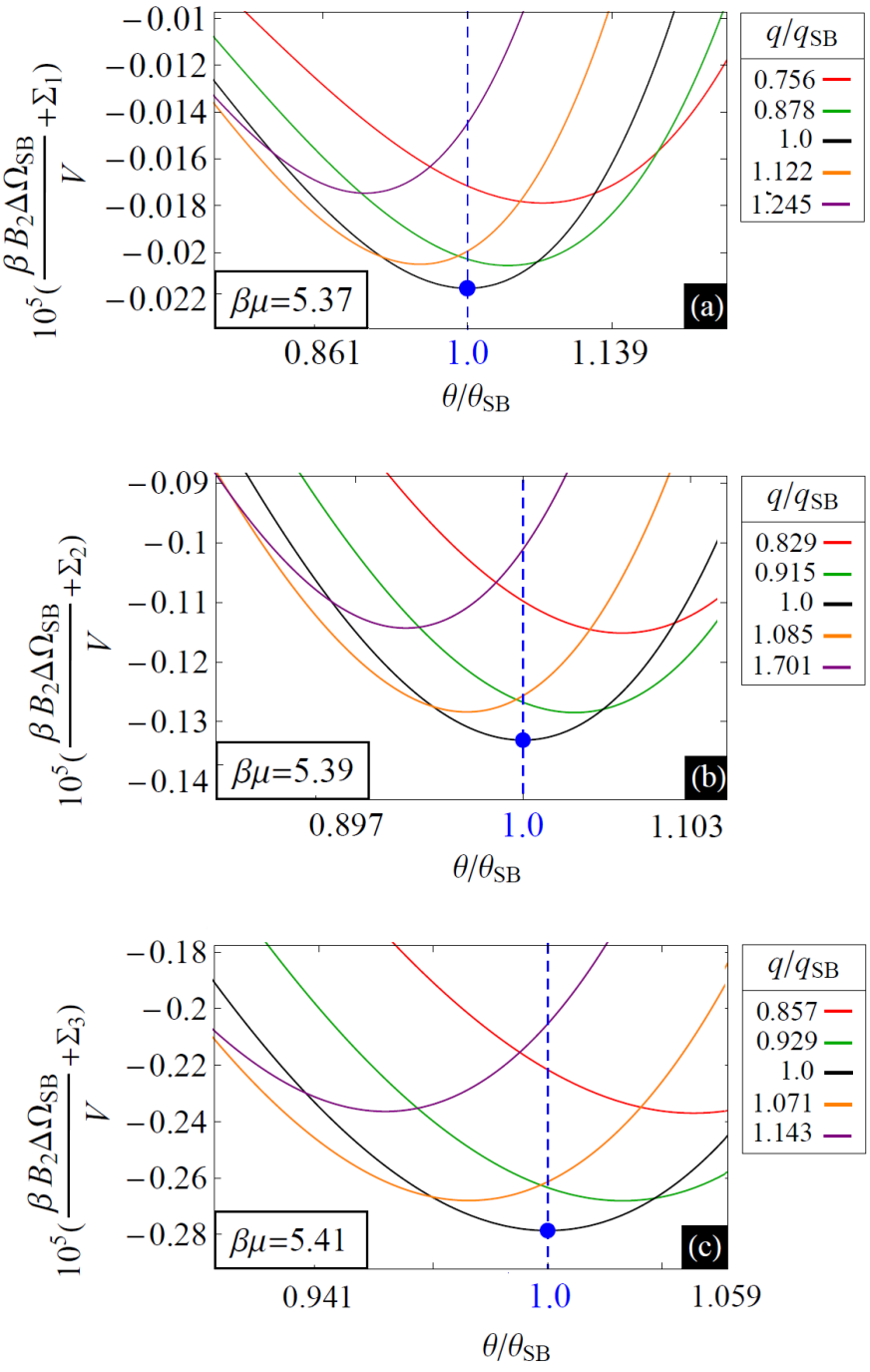

FIG. S6: $\Delta\Omega_{\rm SB}/V$ as a function of the tilt angle θ for several values of the wave number q, in the case of $\beta\mu = 5.37$ (a), $\beta\mu = 5.39$ (b) and $\beta\mu = 5.41$ (c). We consider the coefficients $l_1 = 0.1L^2, l_2 = 0.0427L^2, e_2 = 1, S_0 = 0.99, e_4 = 0.5, \kappa = 0.3L^2$ and $\lambda = 0.18L^2$. We observe that, at each μ, the minimum values of q and θ correspond to the $q_{\rm SB}$ and $\theta_{\rm SB}$ of Eqs. (S5) and (S6), respectively. In (a), (b), and (c) we plot $\Delta\Omega_{\rm SB}/V$ subtracted by the irrelevant constant values $\Sigma_1 = 0.1248, \Sigma_2 = 0.1456$, and $\Sigma_3 = 0.1668$, respectively.

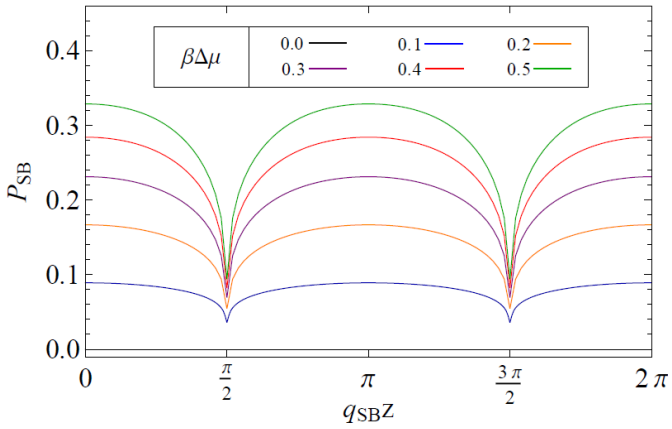

FIG. S7: Amplitude of the polarity $P_{\rm SB}$ in the $N_{\rm SB}$ phase, as a function of z, for the same values of $\Delta\mu \equiv \mu - \mu_{NN_{\rm SB}}$ and of the Landau coefficients as in Fig. 1 of the main text. We observe that $P_{\rm SB}$ is constant along z for $z \leq \mu_{NN_{\rm SB}}$, while it displays modulations along z for $z > \mu_{NN_{\rm SB}}$.

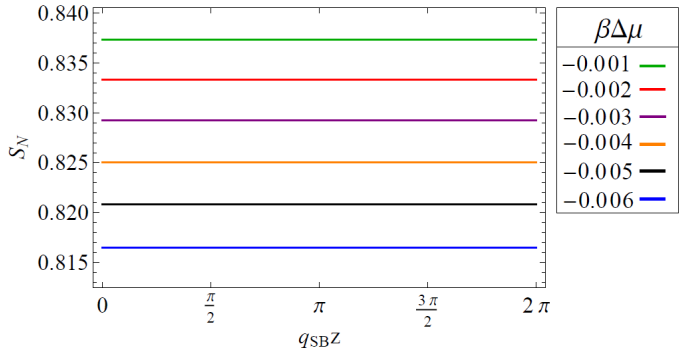

FIG. S8: Nematic order parameter S_N as a function of z, for the same values of the Landau coefficients as in Fig. 1 of the main text, but for several negative values of $\Delta\mu \equiv \mu - \mu_{NN_{\rm SB}} < 0$ (i.e. before the N-$N_{\rm SB}$ transition). We observe that S_N is always constant along z.

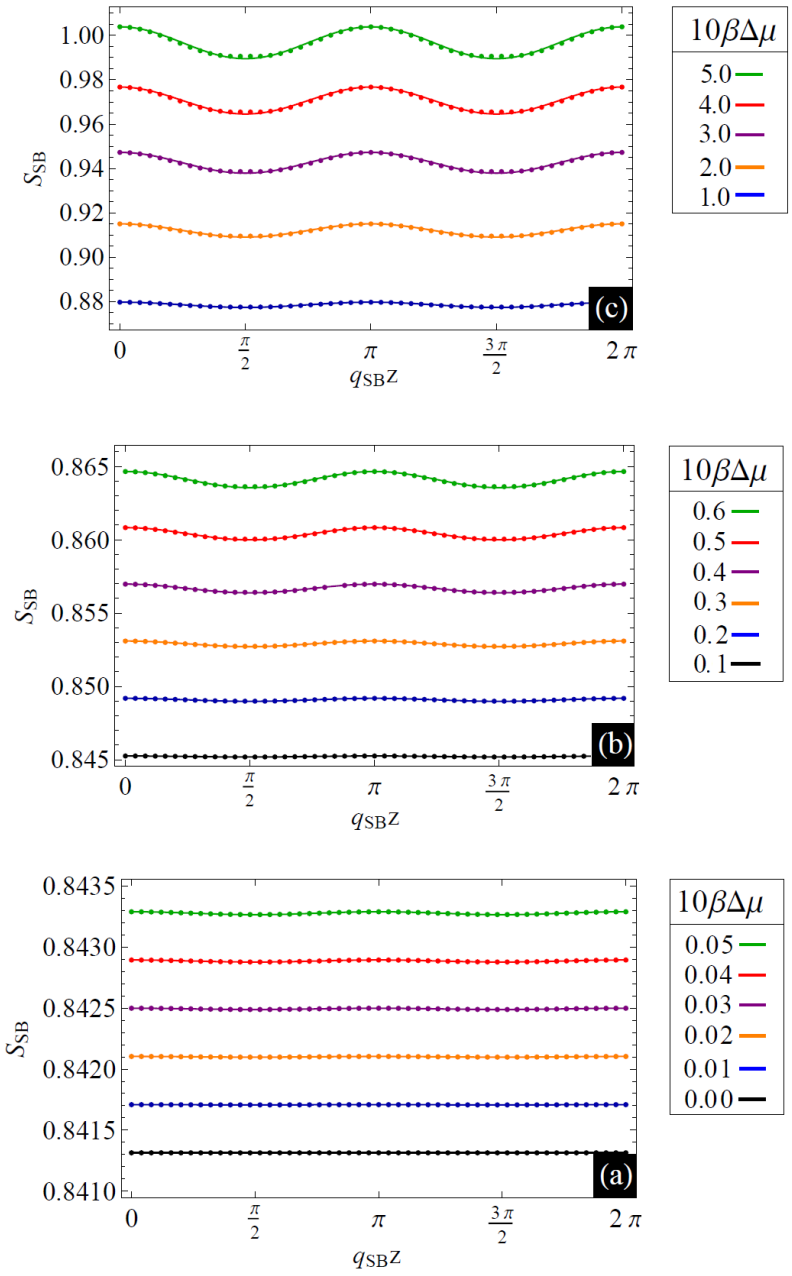

FIG. S9: With full lines we plot the scalar nematic order parameter $S_{\rm SB}$ as a function of $z \in [0, 2\pi/q_{\rm SB}]$ for a large number of $\Delta\mu \equiv \mu - \mu_{NN_{\rm SB}}$, and for the same Landau coefficients as in Fig. 1 of the main text. With points we plot a fit of the numerical results. The fitting function corresponds to Eq. (S7), with coefficient θ_S given in Table S1. Optimum agreement can be observed.

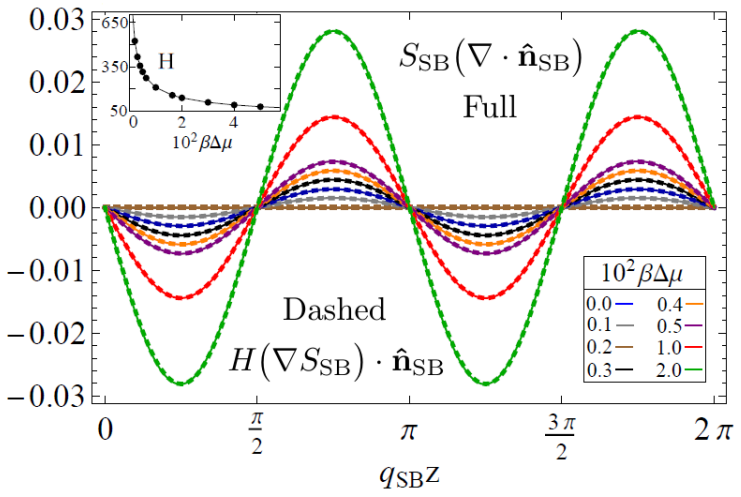

FIG. S10: $S_{SB}(\nabla \cdot \hat{\mathbf{n}}_{SB})$ (full lines) and $H(\nabla S_{SB}) \cdot \hat{\mathbf{n}}_{SB}$ (dashed lines) as a function of z, for several values of the chemical potential $\Delta\mu \equiv \mu - \mu_{NN_{SB}}$ and for the same coefficients as in Fig. 1 of the main text. The fit parameter H varies with μ, as shown in the inset. At each μ, the relation $S_{SB}(\nabla \cdot \hat{\mathbf{n}}_{SB}) = H(\nabla S_{SB}) \cdot \hat{\mathbf{n}}_{SB}$ holds.